Veit Wiesmann*, Dorothea Reimer, Daniela Franz, Hanna Hüttmayer, Dirk Mielenz, and Thomas Wittenberg

Automated high-throughput analysis of B cell spreading on immobilized antibodies with whole slide imaging

Abstract: Automated image processing methods enable objective, reproducible and high quality analysis of fluorescent cell images in a reasonable amount of time. Therefore, we propose the application of image processing pipelines based on established segmentation algorithms which can handle massive amounts of whole slide imaging data of multiple fluorescent labeled cells. After automated parameter adaption the segmentation pipelines provide high quality cell delineations revealing significant differences in the spreading of B cells: LPS-activated B cells spread significantly less on anti CD19 mAb than on anti BCR mAb and both processes could be inhibited by the F-actin destabilizing drug Cytochalasin D. Moreover, anti CD19 mAb induce a more symmetrical spreading than anti BCR mAb as reflected by the higher cell circularity.

Keywords: automated image analysis, whole slide scanning, high-throughput analysis, B cell receptor, spreading

DOI: 10.1515/CDBME-2015-0057

1 Introduction

In the life sciences, various light microscopy techniques are currently employed for the visual assessment, observation and quantification of changes in cell morphology during cell spreading experiments. Typically, such experiments include the acquisition of images at different points in time (time lapse experiments) or the analysis and comparison of different experiment.

For such high-throughput analysis experiments, the whole slide scanning technologies enable experimentalists to acquire massive amounts of multiple-stainded fluorescence images with a high quality. Manual assessment

*Corresponding Author: Veit Wiesmann, Daniela Franz, Hanna Hüttmayer, Thomas Wittenberg: Image Processing and Medical Engineering Department, Fraunhofer Institute for Integrated Circuits IIS, Erlangen, Germany, E-mail: veit.wiesmann@iis.fraunhofer.de Dorothea Reimer, Dirk Mielenz: Division of Molecular Immunology, Department of Internal Medicine III, Nikolaus Fiebiger Center, University Hospital Erlangen and Friedrich-Alexander University Erlangen-Nuremberg, Germany

of these amounts of micrographs is a tedious and time consuming task. Therefore, the application of automated image processing and analysis algorithms is strongly required to solve tasks like cell detection and and nuclei and plasma segmentation in adequate amount of time. It simultaneously increases quality, objectiveness and reproducibility of these experiments.

We combine fluorescence, whole slide imaging with automated image analysis to investigate B cell spreading during the interaction with antigen presenting cells (APC). B cells are lymphocytes of the adaptive immune system.

In the past, various methods for cells and nuclei segmentation in fluorescence microscopy images have been proposed. Most commonly, these methods incorporate thresholding methods for figure-ground separation as well as the watershed transform [12] for object spitting [1, 11, 13]. Alternative approaches apply level sets [2] or are based on the graph cut algorithm [8].

Nevertheless, for each new image analysis application a new set of methods and an adequate processing pipeline has to be established and the corresponding parameters of each part of the pipeline have to be fine-tuned and adapted to the experiments. In contrast to a manual parameter tuning, we adjust parameters with an automated adatpion scheme, which is based on small but representative set of manually labeled cells [7].

2 Materials and methods

Our line of action consists of three steps. First step is the preparation of the B cells on a well slide (cf. Section 2.1). The slides are then captured with a fluorescence whole slide scanner (cf. Section 2.2). Finally, the acquired fluorescence micrographs are automatically analyzed with adequate image processing methods (cf. Section 2.3).

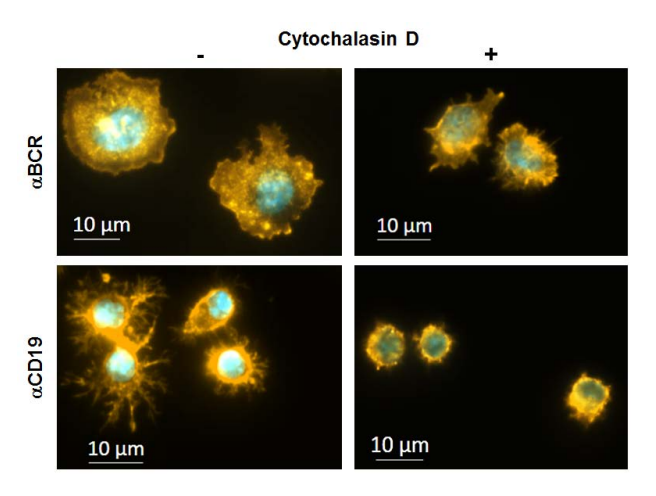


Figure 1: Different cell spreading behavior of LPS activated B cells treated with (right) or without (left) Cytochalasin D on immobilized antibodies α BCR or α CD19.)). Immunofluorescent staining was performed for F-Actin (Phalloidin-Rhodamin) and DNA (DAPI).

2.1 Samples

Naive murine B cells from C57Bl/6 mice were isolated from the spleen by negative selection and activated with lipopolysaccharide (LPS, 10 µg/ml) for 72h in RPMI1640 medium supplemented with fetal calf serum (FCS)(10%), L-glutamine (2 mM), Pyruvate (1 mM), Penicillin (50 U/ml), Streptomycin (50 μ g/ml) and β -Mercaptoethanol (50 μ M). Teflon-coated microscope slides with 8 wells each and a thickness of 6 mm were prepared for coating with α BCR (10µg/ml rat anti BCR monoclonal) [3] or α CD19 (rat anti CD19 monoclonal) [10]. Per well, $2x10^4$ B cells (in 25 μ l volume) were seeded on the coated slides and incubated for 45min in a humidified incubator (5% CO2 atmosphere in RPMI1640 supplemented as described above but without FCS). As a control, B cells were treated with Cytochalasin D [5], a mycotoxin that inhibits actin polymerization. Cell spreading was stopped by fixating the cells in phosphate buffered saline (PBS) containing 4% para-formaldehyde. Fixed cells were washed and permeabilized in PBS with 0.1% Triton X-100. F-actin was specifically stained intracellularly with Phalloidin-Rhodamin (Molecular Probes) and nuclei were stained with DAPI (Roth). Slides were mounted in MOWIOL(Roth).

2.2 Imaging

Each well was automatically recorded with around 25 visual fields and two fluorescent dyes with an Axio Scan.Z1 whole slide scanning fluorescence microscope (Zeiss). The DAPI stained nuclei were used to generate the focus map for each individual well. Then all images were acquired with two fluorescent channels, namely in DAPI for the cell nuclei and Phalloidin-Rhodamin for the cell F-Actin cvtoskeleton. Each micrograph has a spatial resolution of 1388 pixels × 1040 pixels, where the physical pixel size is $0.163 \, \mu m \times 0.163 \, \mu m$. Wells with exceedingly high cell density were neglected and excluded for further analysis. In total, we acquired 7 slides and used 48 wells and 2418 images for further analysis. Fig. 1 shows exemplary parts of recorded images from different conditions.

2.3 Image analysis

The key issue during an automated cell image analysis is an appropriate segmentation of the cell regions. Usually this includes preprocessing the image (preprocessing), separating foreground pixels from background pixels (figure-ground separation), and, if necessary, separating cells from each other (cell splitting). An additional measurement step for e.g. the assessment of cell area or cell circularity follows cell segmentation. Segmentation and measurements are integrated in the experimental analysis tool (CaeT). CaeT allows to combine various methods with each other to design cell image processing pipelines of arbitrary length. This is a similar approach like in the CellProfiler [4].

In this study, we have applied a combination of various algorithms to nuclei and to cell segmentation. Fig. 2 depicts the segmentation pipeline for nuclei segmentation. Gaussian smoothing filters an image with a Gaussian kernel with the standard deviation σ_n and produces a smoothed version of the original image (preprocessing). The smoothed image is used for figure-ground separation with a method that is based on k-means clustering with one parameter k_n , the number of clusters [7]. Nuclei splitting is performed with a watershed approach. After smoothing the distance transformed result of the figureground separation with Gaussian smoothing with standard deviation $\sigma_{\rm nd}$, it applies the watershed transfrom and neglects segments with areas smaller than a_n to prevent oversegmentation.

Fig. 3 shows the image processing pipeline for cell segmentation. Preprocessing is performed with a Difference of Gaussians filter (DoG). This filter generates two smoothed



Figure 2: Image processing pipeline for nuclei segmentation.



Figure 3: Image processing pipeline for cell segmentation.

versions of the original image with the Gaussian filter with the standard deviations σ_c and σ_{cb} . The foreground of the micrograph is estimated by subtracting these smoothed images from each other. Figure-ground separation is performed with k-means clustering with the number of clusters k_c on the result of the DoG. Now, the seeded watershed algorithm is used for cell splitting and uses the previously detected nuclei regions as starting point for the watershed transform. Parameters are $\sigma_{\rm cd}$ for smoothing the distance transformed image and a_c determining the minimum cell size.

In order to obtain the best result fro the image analysis challenge, all parameters $\mathbf{p} = (\sigma_n, k_n, \sigma_{nd}, a_n, \sigma_c, \sigma_{cb}, k_c,$ $\sigma_{\rm cd}$, $a_{\rm c}$) of all methods applied within the image processing pipeline have to be adapted to the experimental image data. For human experts, this is an elaborate and timeconsuming task. Held et al. [9] have presented a method to automatically optimize parameters of a three-step image processing pipeline with respect to a small set of hand labeled reference image data. In this contribution this approach has been extended to adapt the parameters of image processing pipelines with arbitrary length. The optimization algorithm makes use of coordinate descend approach in order to find the best fitting parameter set \mathbf{p}^* using the combined Jaccard metric presented in [9] as optimization measure. To provide the ground truth data for the parameter optimization, a subset of 15 representative images with 149 cells and 165 nuclei, respectively, were manually labeled by an human expert using a Wacom Board [6]. Incomplete cells and nuclei witch contact to image tile borders were excluded.

3 Results

In order to process the described whole slide image data, an appropriate parameter set \mathbf{p}^* has to be found for each image processing pipelines. These parameters are separately adapted for the nuclei segmentation pipeline (see fig. 2) and for the F-actin cytoskeleton segmentation pipeline (see fig. 3) with respect to the hand labeled reference image data. As segmented nuclei regions are input into the F-actin cytoskeleton pipeline, the parameter set for the nuclei segmentation is the first to be adapted. For nuclei, the performance measured with two-fold cross val-

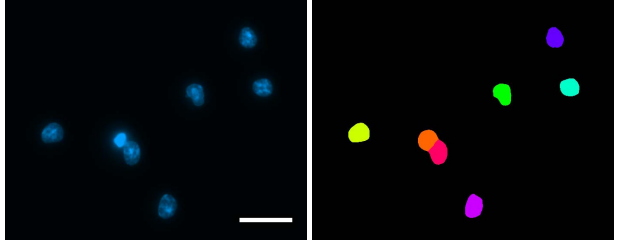


Figure 4: Exemplary segmentation result for nuclei: part of original DAPI image (left); segmentation result (right); scale bar corresponds to 20 μ m.

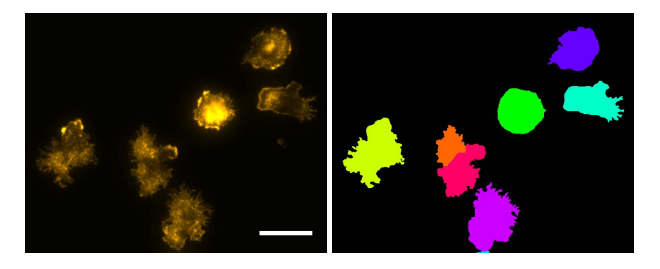


Figure 5: Exemplary segmentation result for F-actin cytoskeleton: brightness adapted part of original Phalloidin-Rhodamin image (left); segmentation result (right); scale bar corresponds to 20 µm.

idation and the combined Jaccard metric is p_n =0.73 with a hit quality of h_n =0.91. Fig. 4 shows an exemplary segmentation result. For F-actin cytoskeleton, the performance was p_c =0.64 with a hit quality h_c =0.84. Fig. 5 depicts an exemplary segmentation.

The quality measures based on the combined Jaccard index are affected by differences between human labeling and automated image processing. The automated process uses the DAPI channel as a reference channel and tries to delineate exactly one cell region for each detected nucleus region. In contrast, a human expert's decision depends more on the channel currently depected. This means if the staining works fine in the DAPI channel the human expert might have delineated a nucleus although there is not a visible cell in the F-actin cytoskeleton channel and vice versa. Also, the human experts were able to recognize dividing nuclei based on the F-actin cytoskeleton channel, and have labeled the nucleus as a single one. However, the algorithm separates the nucleus into two entities if the division process is sufficiently advanced and two distinct nuclei ca be detected. There also exist differences in the handling of debris and dirt in the micrograph. Human experts are able to distinguish between dirt, debris and cells based on morphology and texture, while the algorithm is only able to sort out too small regions.

With the parameters obtained during the optimization process the complete experimental image data was processed. This resulted in a total number of 16.715 de-

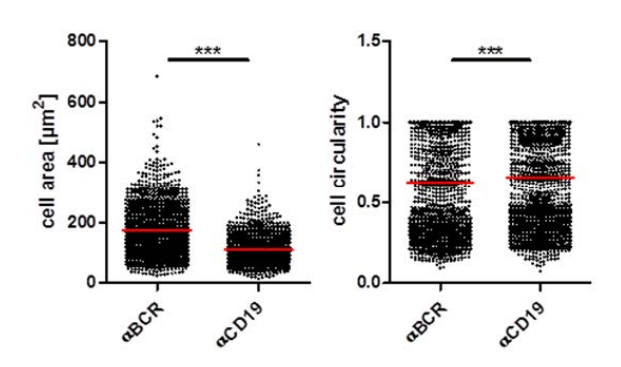


Figure 6: Measurements depict highly significant results in cell area and circularity between B cells spreading on immobilized α BCR or α CD19 antibodies. Significance according to Mann-Whitney-U test (*** p= 0.0001 - 0.001). Red line represents the mean.

tected and segmented cells and nuclei, respectively. Based on the segmented cell regions, the cell area and the cell circularity were calculated to describe the morphology of each cell. The results are visualized in fig. 6. The analysis shows that LPS-activated primary murine B cells, attached on glass slides coated either with anti BCR mAb, or coated with antibodies against the BCR co-receptor CD19, in the absence (-) or in the presence of the F-actin destabilizing drug Cytochalasin D, spread significantly less on anti CD19 mAb than on anti BCR mAb. The F-Actin dependency of both processes could be shown via specific inhibition by Cytochalasin D. Furthermore, anti CD19 mAb induce a more symmetrical spreading of B lymphocytes than anti BCR mAb as reflected by the significant higher cell circularity.

4 Conclusion

In summary, we have established a protocol and an algorithm that allows the quantification of large numbers of fluorescent labeled and fixed B cells attached to glass slides. This method allows rapid screening of cytoskeletal effector molecules and of mouse mutants suspected to effect cytoskeletal rearrangement.

Acknowledgment: This work has been supported by the Collaborative Research Center 796 Project A4 and transregional collaborative research center 130 TP03. Both research centers are funded by the German Research Foundation.

Author's Statement

Conflict of interest: Authors state no conflict of interest.

Material and Methods: Informed consent: Informed consent has been obtained from all individuals included in this study. Ethical approval: The research related to human use has been complied with all the relevant national regulations, institutional policies and in accordance the tenets of the Helsinki Declaration, and has been approved by the authors' institutional review board or equivalent committee.

References

- Bengtsson EC, Wählby C. Robust cell image segmentation methods. Pattern Recognition and Image Analysis. 2004; 14(2):157-167.
- [2] Bunyak F, Palaniappan K, Nath SK, Baskin TI, Dong G. Quantitative cell motility for in vitro wound healing using level set-based active contour tracking. Proc IEEE Int Symp Biomed Imaging. 2006; 6:1040-1043.
- [3] Cambier JC, Heusser CH, Julius MH. Abortive activation of B lymphocytes by monoclonal anti-immunoglobulin antibodies. J Immunol. 1986;136(9):3140-6.
- [4] Carpenter AE, Jones TR, Lamprecht MR, et al. CellProfiler: Image Analysis Software for Identifying and Quantifying Cell Phenotypes. Genome Biology. 2007; 7:R100
- [5] Cooper, JA (1987). Effects of cytochalasin and phalloidin on actin. J Cell Biol. 1987; 105(4): 1473–1478.
- [6] Dach C, Held C, Palmisano R, Wittenberg T, Friedl S. Evaluation of input modalities for the interactive image segmentation of fluorescent micrographs. Biomed Tech. 2011; 56 (Suppl. 1).
- Held C. Towards Increased Efficiency and Automation in Fluorescence Micrograph Analysis Based on Hand-Labeled Data. Universität Bielefeld. 2013.
- [8] Held C, Wenzel J, Wiesmann V, Palmisano R, Lang R, Wittenberg T. Enhancing automated micrograph-based evaluation of LPS-stimulated macrophage spreading. Cytometry A. 2013; 83(4):409-18.
- [9] Held C, Nattkemper T, Palmisano R, Wittenberg T. Approaches to automatic parameter fitting in a microscopy image segmentation pipeline: An exploratory parameter space analysis. J Pathol Inform. 2013; 4(Suppl): S5.
- [10] Krop I, Shaffer AL, Fearon DT, Schlissel MS. The signaling activity of murine CD19 is regulated during cell development. J Immunol. 1996;157(1):48-56.
- [11] Malpica N, Ortiz de Solorzano C, Vaquero JJ, et al. Applying watershed algorithms to the segmentation of clustered nuclei. Cytometry. 1997; 28(4):289-297.
- [12] Roerdink JB, Meijster A. The watershed transform: Definitions, algorithms and parallelization strategies. Fundamenta informaticae. 2000; 41. Jg., Nr. 1:187-228.
- [13] Wählby C, Lindblad J, Vondrus M, Bengtsson E, Björkesten L. Algorithms for cytoplasm segmentation of fluorescence labelled cells. Anal Cell Pathol. 2002;24(2-3):101-11.